Conf-9409255--3

PNL-SA-25348

# MEASUREMENT OF THE SEASONAL AND ANNUAL VARIABILITY OF TOTAL COLUMN AEROSOL IN A NORTHEASTERN U.S. NETWORK

J. J. Michalsky[a]
J. A. Schlemmer[a]
N. R. Larson
L. C. Harrison[a]
W. E. Berkheiser III[a]
N. S. Laulainen

September 1994

Presented at the
Speciality Conference on Aerosol and Atmospheric Optics: Radiation Balance and Visual Air Quality
September 25-30, 1994
Snowbird, Utah

Prepared for
the U.S. Department of Energy
under Contract DE-AC06-76RLO 1830

Pacific Northwest Laboratory
Richland, Washington 99352

(a) University of Albany, Albany, New York

# Measurement of the Seasonal and Annual Variability of Total Column Aerosol in a Northeastern U.S. Network

PNL-SA-25348

J.J. Michalsky*, J.A. Schlemmer*, N.R. Larson†, L.C. Harrison*,
William E. Berkheiser III*, and N.S. Laulainen†

Atmospheric Sciences Research Center*
University at Albany, State University of New York
100 Fuller Road
Albany, New York 12205 USA

Pacific Northwest Laboratory†
P.O. Box 999
Richland, Washington 99352 USA

## ABSTRACT

A network of multi-filter rotating shadowband radiometers has operated since late 1991 in the northeastern United States. The data acquired are simultaneous measurements of total and diffuse horizontal irradiances in six narrowband filtered detectors and one broadband shortwave detector. The direct normal irradiances are calculated from these measurements.

These direct data are corrected for cosine response and used to calculate extraterrestrial irradiance ($I_o$) using the Langley method of regressing the natural logarithm of direct irradiance versus air mass. With frequent determinations of $I_o$, changes in $I_o$ caused by soiling and filter degradation, for example, can be tracked.

Using these $I_o$'s, total optical depth is calculated for every clear 30-minute period in the record. Consequently, total optical depth may be obtained on a fair number of days throughout the year. Using daily average total optical depth we have calculated aerosol optical depths for five wavelengths by subtracting Rayleigh scattering optical depths and Chappuis ozone absorption optical depths at each wavelength.

The aerosol pattern at nearly every site is an annual cycle superimposed on a decaying stratospheric loading associated with the Mount Pinatubo volcanic eruption. An attempt is made to remove the volcanic signal using data from another site.

## INTRODUCTION

As part of the Department of Energy's Quantitative Links (QL) Program, a nine-station radiation network was established in the northeastern and mid-western United States. A goal of the QL program is to link global and regional climate change to changes in the mix of atmospheric trace species. The Atmospheric Sciences Research Center (ASRC) and the Pacific Northwest Laboratory (PNL) have been funded by this program to study change in longwave and shortwave radiation that occurs on time scales of minutes to years as a result of aerosol and cloud changes.

The network that was established in late 1991 is shown in figure 1. The sites were selected to be regionally representative of an area with no significant local sources of pollution. The sites are operated by local colleges and universities or government research laboratories who perform routine maintenance and report, or fix, malfunctions in the instruments.

The primary instrument for shortwave radiation measurements in the network is a multi-filter rotating shadowband radiometer (MFRSR), which measures total and diffuse horizontal irradiance, from which direct normal irradiance is calculated.[1] A silicon cell pyranometer is inverted to measure upwelling shortwave radiation, primarily for the detection of snow cover. A pyrgeometer measures downwelling hemispherical longwave radiation. Supplementing these radiation instruments are a rain

gauge, and an ambient temperature/relative humidity probe.

Our stated goals for our involvement in the QL program are (1) to relate cloud and aerosol patterns to upwelling and downwelling shortwave and longwave irradiances, (2) to measure changes in cirrus cloud patterns that are predicted by some models to occur in response to increasing greenhouse gases, and (3) to assess changes in aerosol loading that may result in direct and indirect radiative climate forcing, but opposite in sign to greenhouse warming.[2] This paper focusses on the third of these, which also relates to the visibility problem. We are concerned with detecting changes in regional visibility caused by changes in the tropospheric aerosol patterns with season and from year to year.

The next section describes the MFRSR. That is followed by a discussion of our methodology for tracking aerosol behavior. We finish with a discussion of results and conclusions based on data acquired to date.

## THE MULTI-FILTER ROTATING SHADOWBAND RADIOMETER

The basic geometry of a computer-controlled MFRSR can be seen in figure 2. The shadowing band is a strip of metal formed into a circular arc that lies along a celestial meridian (the face of the Lambertian detector is the center of this arc). It can be precisely rotated (0.4°) around the polar axis by a stepping-motor that is in turn controlled by a microprocessor. This band blocks a strip of sky with an umbral angle of 3.27°, more than sufficient to block the solar disk. The mechanism permits a simple mechanical adjustment for the latitude. This adjustment, together with the azimuth alignment to the earth's pole, is done when the instrument is installed at a site, and no further mechanical adjustment is necessary.

The operation of the instrument is controlled by its self-contained microprocessor. At each measurement interval it computes the solar position using an approximation for the solar ephemeris. The measurement sequence starts with a measurement made while the band is at the nadir; this is the total horizontal irradiance. The band is then rotated to make three measurements in sequence: the middle one blocks the sun and the other two block strips of sky 9° to either side. These side measurements permit a first-order correction for the "excess skylight" blocked by the band when the sun-blocking measurement is made; the average of these two side measurements is subtracted from the total horizontal measurement; this correction is then added to the sun-blocked measurement to determine the diffuse horizontal irradiance. Finally, the diffuse component of the irradiance can be subtracted from the total horizontal to produce the direct horizontal component. Division by the cosine of the solar-zenith angle (available from the ephemeris calculation) then produces the direct beam flux on a normal surface. The entire measurement sequence is completed in less than ten seconds and is normally programmed to occur four times per minute.

The optical inlet is a protruding diffuser surrounded by a raised blocking ring. The diffuser is made of Spectralon®, an optical plastic manufactured by Labsphere, Inc. The thin-walled external "button" acts as a transmission diffuser, and the thick internal sidewalls form a partial integrating cavity. Two diaphragms of frosted Schott Glass Technologies WG-280 glass act as transmission diffusers to increase the randomization of the photon trajectories. The entire detector consists of the diffuser-integrator that illuminates an internal hexagonal close-packed array of seven photodiodes with interference filters. The interior of the detector assembly is thermally insulated, and has a thermostatic electrical heater that holds the temperature of the internal detector assembly at a setpoint chosen between 35° C to 45° C. The MFRSR instruments built for the QL program have six filtered detectors with nominal 10 nm full width at half maximum (FWHM) bandwidths at wavelengths of 415, 500, 610, 665, 862, and 940 nm and an unfiltered silicon photodiode. All the filtered passbands except 940 nm (a water vapor band) are chosen to permit Langley analysis for the direct determination of optical depth. The wavelengths were chosen to span a useful range for flux calculations, and to permit the maximum information about the aerosol to be retrieved via inversions such as those described by King et al.[3]

## AEROSOL MEASUREMENT METHODOLOGY

### Data Retrieval

In the QL instruments samples are taken every 15 seconds, and 20 of these samples are recorded as a five-minute average. All data are retrieved via modem every two days although the memory will hold more than three days' data for a QL instrument suite measuring data at five-minute intervals.

### Cosine Correction

The direct irradiance data are corrected for imperfect cosine response after they are down-loaded. Before the MFRSR goes into the field its angular response is measured using our cosine-response bench.[4] A $2\pi$ steradian detector's response should be symmetric with respect to azimuth and decrease as the cosine of the incident angle measured from the direction normal to the detector face. Its departure from this perfect response is measured and used to correct retrieved data. After the direct is corrected, a corrected total horizontal irradiance is calculated by summing the corrected direct horizontal component and the diffuse horizontal. The direct data are used for Langley plots.

### Langley Analysis

Optical depths are derived using Langley analysis. The assumption is made that the measured extinction in the five filters that we are using follows the Bouguer-Lambert-Beer law, i.e.,

$$I = I_o * \exp(-\tau * m) \qquad (1)$$

where

- $I$ = measured direct irradiance
- $I_o$ = direct irradiance at the top of the atmosphere
- $\tau$ = total optical depth
- $m$ = air mass relative to zenith direction.

If we take the natural logarithm of both sides of equation (1), we get

$$\ln(I) = \ln(I_o) - \tau * m. \qquad (2)$$

Plotting the ln(I) versus m produces a linear plot with a negative slope of $\tau$ and an intercept of $\ln(I_o)$. This procedure is illustrated in figure 3. The solid line is a linear least squares fit to the data.

In our northeastern and mid-western U.S. sites the atmosphere is unstable relative to mountain sites in the western U.S. Consequently, the $I_o$'s are not reproducible from day to day to high precision. However, they are consistent enough that averaging yields a robust estimate of the true $I_o$. This has been confirmed by comparing the averaged $I_o$ just after field deployment with standard light calibrations of the instrument just before field deployment. The agreement was within the 4% accuracy quoted for the lamp spectral irradiance for all five filters used for aerosol derivation.

Because of soiling and filter drifts and repairs necessitating adjustments to the filter head, $I_o$'s can change (see figure 4). It has been our experience that they either do not change within the accuracy of the $I_o$ variations or the drift is linear with time and can be so approximated. We have used a median $I_o$ or an $I_o$ that varies linearly in time for each of the filters along with equation (1) to calculate total optical depth.

Thirty-minute times series of total optical depths, calculated as above, are formed and fit with a linear function in time. If no single point lies outside 0.01 optical depths, then an average optical depth is calculated for this 30-minute period and the next 30-minute time series is considered. If there is an outlier according to this strict criterion, then the time series is advanced five minutes, and the test is repeated. This procedure allows the aerosol optical depth to change slowly with time, but

sub-visual cirrus obscuration is excluded by this procedure.

In this analysis we are interested in seasonal and annual changes, therefore, we formed daily averages from all 30-minute data intervals for a particulate day. This minimizes the extra weighting that would be assigned to the clearest days in the time series that we are to consider in the analysis that follows.

Before we proceed we need aerosol optical depth. The total optical depth for the five filters that we have chosen for this analysis is the sum of components as indicated in equation (3).

$$\tau_{total} = \tau_{Rayleigh} + \tau_{ozone} + \tau_{aerosol} \qquad (3)$$

where

$\tau_{total}$ = total optical depth from the Langley analysis
$\tau_{Rayleigh}$ = Rayleigh scattering optical depth for each wavelength corrected for pressure
$\tau_{ozone}$ = Chappuis-band ozone absorption optical depth using seasonal ozone estimates
$\tau_{aerosol}$ = aerosol scattering and absorption optical depth.

We subtract mean, pressure-corrected Rayleigh optical depth and long-term, average ozone optical depths for the site in this paper although in the future we expect to use actual pressure and better estimates of total column ozone for these corrections. We suspect that we may be in error by a few thousandths of an optical depth by not using better corrections.

## RESULTS

Figure 5 is a plot of 450 daily averages of aerosol optical depth at 500 nm from the ASRC QL site. The data cover a period of a little more than two and one-half years. The solid line on this plot is a smoothing function known as locally-weighted, robust regression, also called lowess.[5] The number of points included in the estimate is chosen by the analyst. In this case it includes all points within about a three-month window; however, points included in the estimate are weighted by their proximity to the point in time for which the estimate is required. The lowess smoother, in addition, gives less weight to points distant in value from the optical depth estimate even if a point is very near in time. This prevents extremely high or low turbidity points that are short-lived from exerting much influence on the estimate.

From the points and especially the lowess estimate we see an overall decrease each succeeding year. The extreme jump near the end of the data is associated with an artifact of the lowess procedure. Its high value depends on very few high aerosol optical depth values in the summer and should be ignored. It is very difficult to discern the seasonal aerosol behavior in the troposphere from this plot. Mount Pinatubo erupted in June 1991, and its effects are still felt at mid-northern latitudes. Typically, summers have the highest aerosol optical depth and winters are the lowest. The volcanic pattern is opposed to the tropospheric one for mid-latitudes in that the highest optical depths are in the winter and lowest in the summer. The net pattern depends on the relative contributions of each. The highest lowess estimate occurs in late winter in each of the years shown.

Figure 6 is a plot of 399 points for the University of Maine site. The data and lowess estimate are very similar to figure 5. The ASRC and Maine sites are relative clean sites for locations east of the Mississippi River.

Figure 7 is a plot for of 373 days at Bluefield State College in southern West Virginia. It is distinguishable from the first two sites by its very hazy summers that appear to show an increasing trend, although the summer of 1994 increase is partially a lowess artifact as discussed earlier.

Figure 8 illustrates a problem. The Champagne, Illinois, site operated by the Illinois State Water Survey experiences frequent storms with lightning in the summer months. A combination of a nearby strike and difficulty in getting spare parts put this site out of commission during the summer of 1993. We can tell that there is overall improvement between 1992 and 1994, but we are uncertain about the middle of 1993, which would have been an interesting case study because of the extremely

wet conditions that year. The edge effects associated with the lowess estimate in the summer 1993 gap should be ignored as discussed earlier.

## Mount Pinatubo

Michalsky et al.[6] discuss a procedure for estimating the vertical column aerosol loading of the atmosphere by the Mexican volcano El Chichon. Before the eruption the stratosphere is clean, and the data are overplotted as a function of time of the year and a lowess estimate is derived for this background seasonal variation assuming there is reproducible aerosol behavior during the time that the background data are acquired. The data after the eruption have these seasonal background aerosol optical depths subtracted, and this differenced data set has a lowess estimate made to it that represents the estimate of net loading to the atmosphere by the volcanic eruption.

Aerosol optical depth data at a wavelength of 550 nm have been acquired from a single channel rotating shadowband radiometer since 1989 in Boulder, Colorado. Since data were available before the eruption of Mount Pinatubo, a background seasonal aerosol load can be established. When this background is subtracted from the entire data set, we have an estimate of the Pinatubo aerosol loading as a function of time for that site. It is expected that Albany at a latitude of about 43° and Boulder at a latitude of 40° will, on a seasonally-averaged basis, experience nearly the same aerosol loading resulting from the Pinatubo volcanic eruption.

To the extent that the Pinatubo aerosol above Boulder and Albany are similar, we have derived an estimate for the Albany background aerosol variation over the past two and one-half years. We subtract the lowess estimate of Mount Pinatubo aerosol as a function of time from the individual data points and use a lowess fit to the resulting points to estimate the background aerosol as a function of time. This estimate with Pinatubo aerosol removed is shown in figure 9. The seasonal data look fairly consistent from year to year with peaks in the summer and winter minima as expected.

## CONCLUSIONS

Although the northeastern and mid-western United States is not considered a good place to use sun photometry for the measurement of aerosol optical depths, we believe that we have shown that it is possible with automated, continuous measurements to obtain a reasonable representation of the seasonal and annual changes in aerosol load in the atmosphere. In a little more than two and one-half years, approximately 400 daily average values of aerosol optical depth were calculated for each site, and data were distributed fairly uniformly throughout the year.

To get accurate results, we used all available Langley plots to estimate extraterrestrial irradiance. These $I_o$'s allowed us to track calibration changes caused by filter drift, soiling, etc.

It is preferable, although not always possible, to have a near continuous record with equipment breakdowns repaired quickly. Long breaks in the record complicate the analysis of seasonal and longer-term changes.

Volcanic eruptions further complicate the analysis of tropospheric change since our measurement is of total column aerosol. Even in the northeastern and mid-western U.S., where turbidity is high, the effect of Mount Pinatubo is easily discerned in the data record. The removal of Mount Pinatubo effects using data from a site at the same latitude can yield a fair approximation of the tropospheric aerosol optical depth and, hence, visibility.

It is our proposition, based on these results, that carefully monitored automated measurements can yield a definitive answer to whether aerosol loads change if the data are collected over a long period and volcanic perturbations are independently measured.


## Acknowledgments

This research was supported by the U.S. Department of Energy's Quantitative Links Program through a subcontract with PNL and by the Atmospheric Radiation Measurements Program through grant number DE-FG02-90ER61072. Both programs are within the Office of Health and

Environmental Research. PNL is operated for the Department of Energy by Battelle Memorial Institute under contract DE-AC0676RLO 1830.

## References

(1) Harrison, L.; Michalsky, J.; Berndt, J. Appl. Opt. **1994** 33, 5118-5125.

(2) Charlson, R.J.; Schwartz, S.E.; Hales, J.M.; Cess, R.D.; Coakley, J.A., Jr.; Hansen, J.E.; Hofmann, D.J. Science **1992** 255, 423-430.

(3) King, M.D.; Byrne, D.M.; Herman, B.M.; Reagan, J.A. J. Atmos. Sci. **1978** 35, 2153-2167.

(4) Michalsky, J.J., Harrison, L.C., and Berkheiser, W.E. III, "Cosine Response Characteristics of Radiometric and Photometric Sensors," in *Proceedings of the 1992 Annual Conference of the American Solar Energy Society,* American Solar Energy Society, Boulder, Colorado, 1992; pp. 335-339.

(5) Cleveland, W.S. J. AM. Stat. Assoc. **1979** 74, 829-836.

(6) Michalsky, J.J.; Pearson, E.W.; LeBaron, B.A. J. Geophy. Res. **1990** 95, 5677-5688.


Figure 1. Quantitative Links network sites.

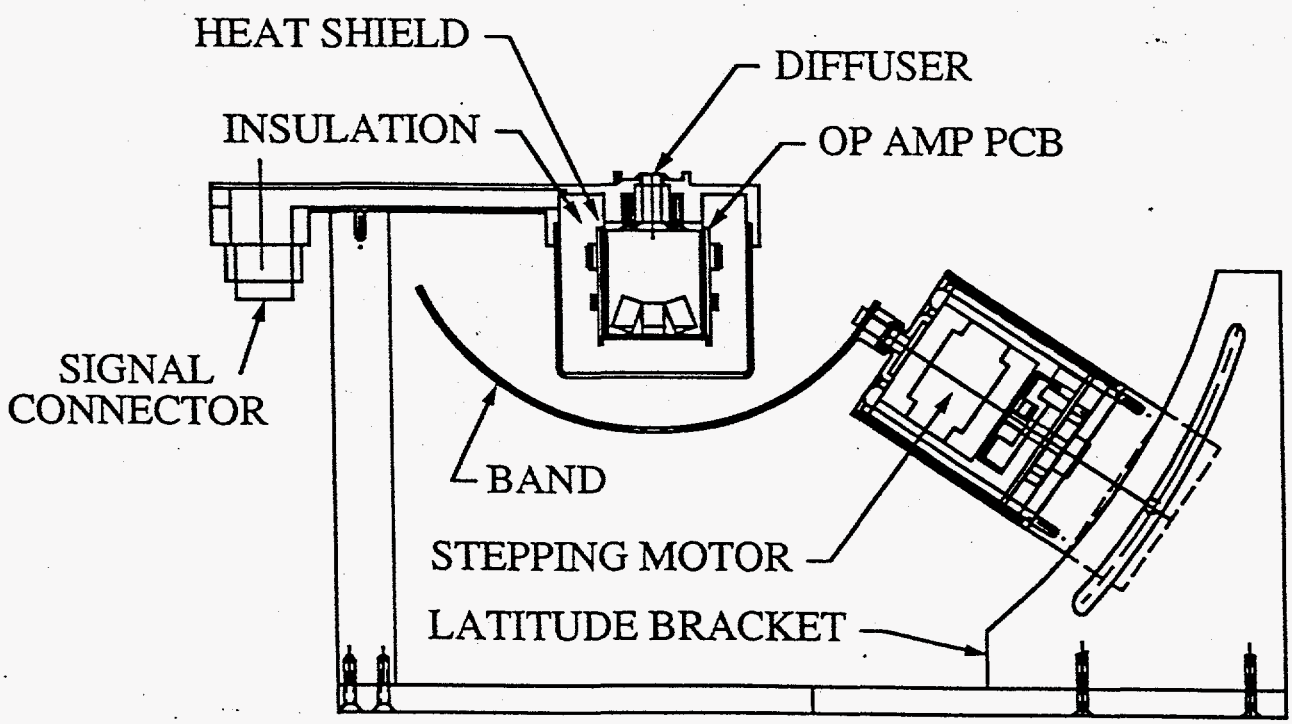


Figure 2. Multi-filter rotating shadowband radiometer.

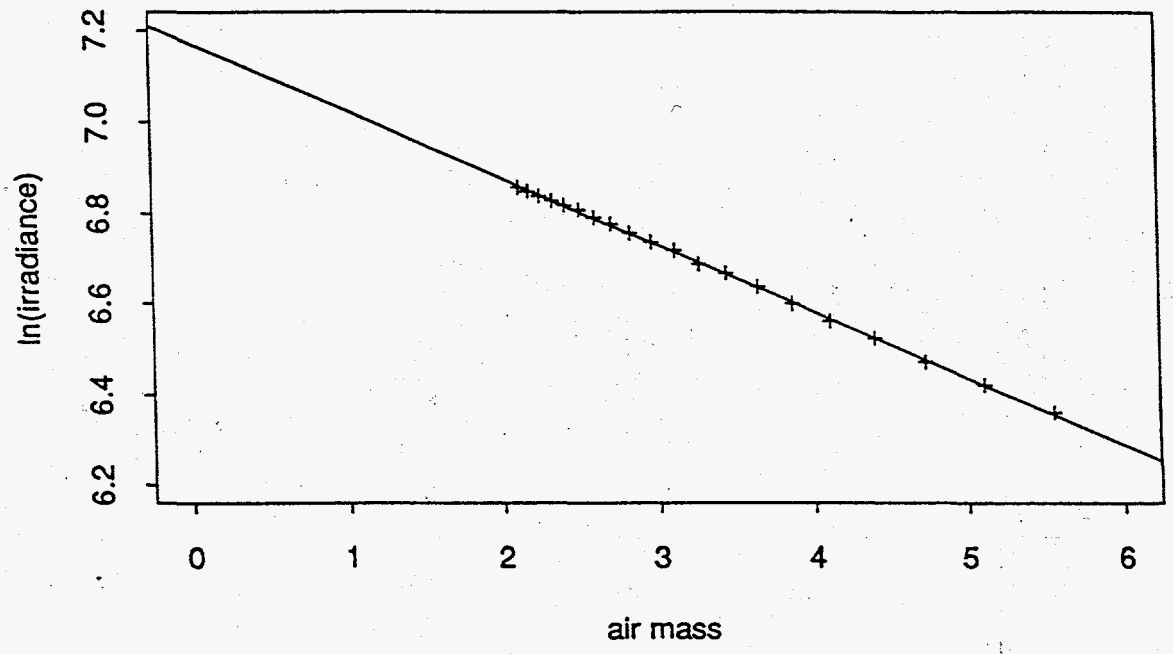


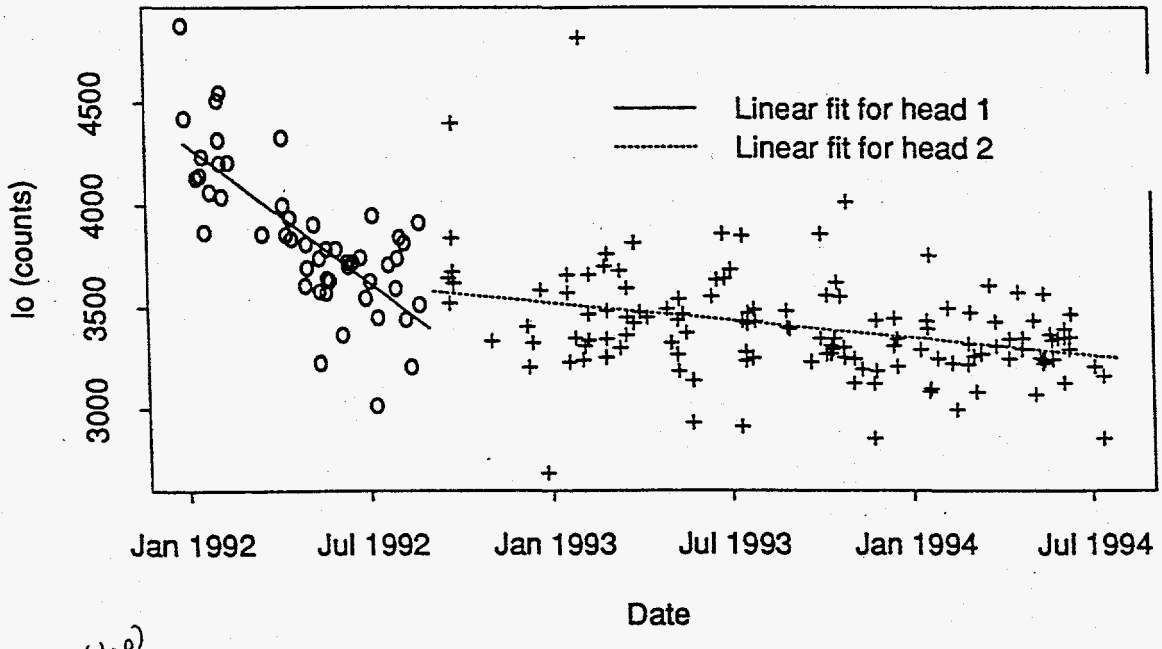


(top)

Figure 3. Langley plot of natural log irradiance vs air mass. Intercept is top-of-atmosphere irradiance estimate and slope is estimated optical depth.

(bottom)

Figure 4. Linear trends in $I_o$ caused by detector adjustment, filter drift, or soiling.

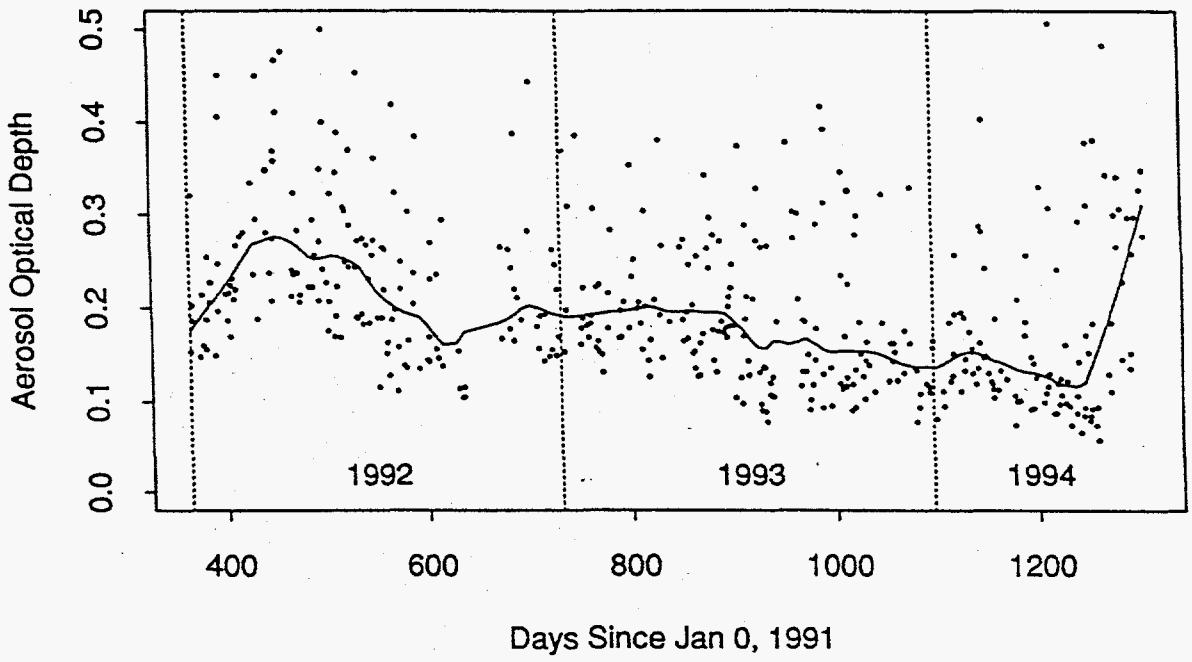


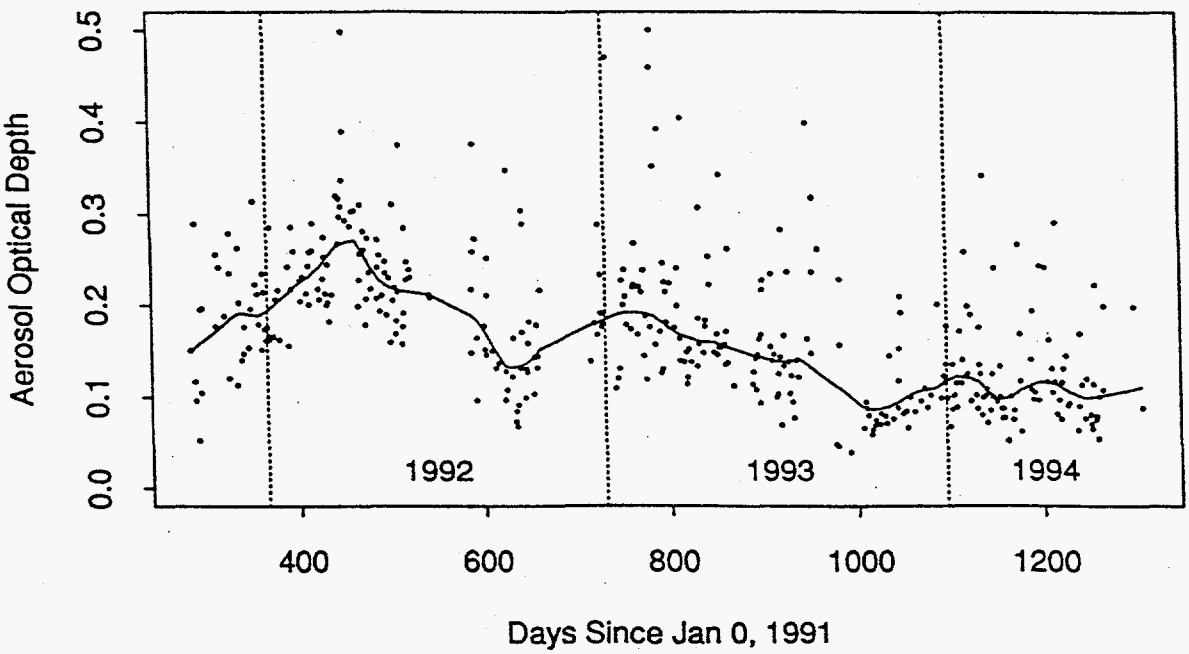


Figure 5 (top). Aerosol optical depth time series for ASRC at 500 nm.
Figure 6 (bottom). Aerosol optical depth time series for University of Maine at 500 nm.

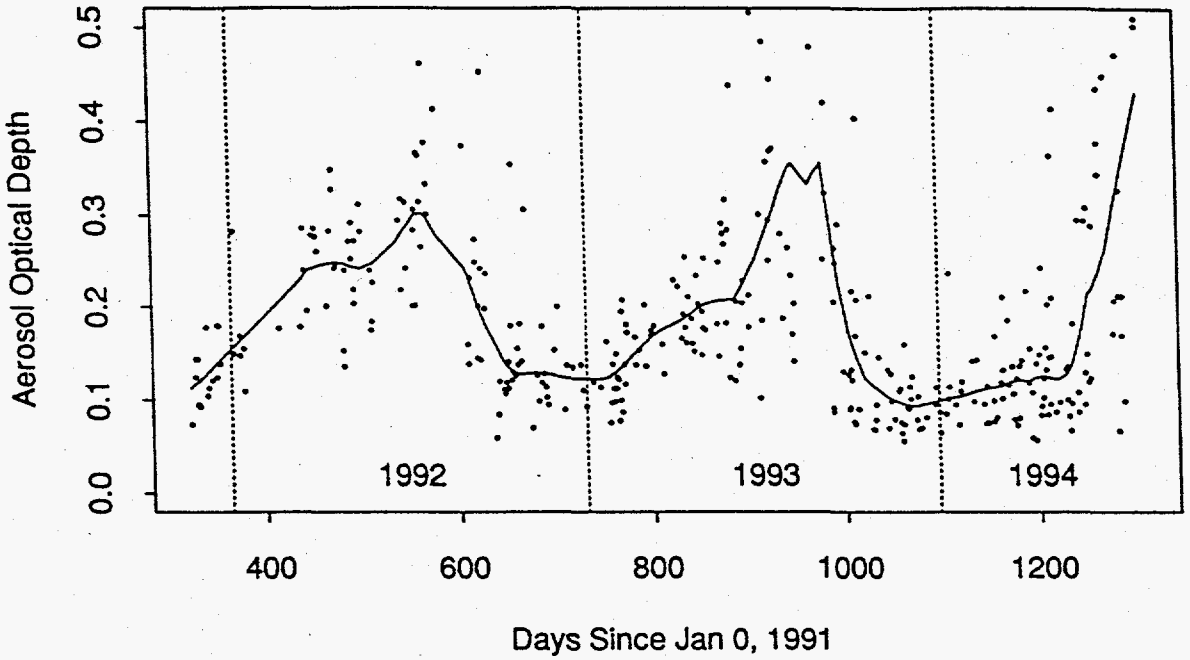


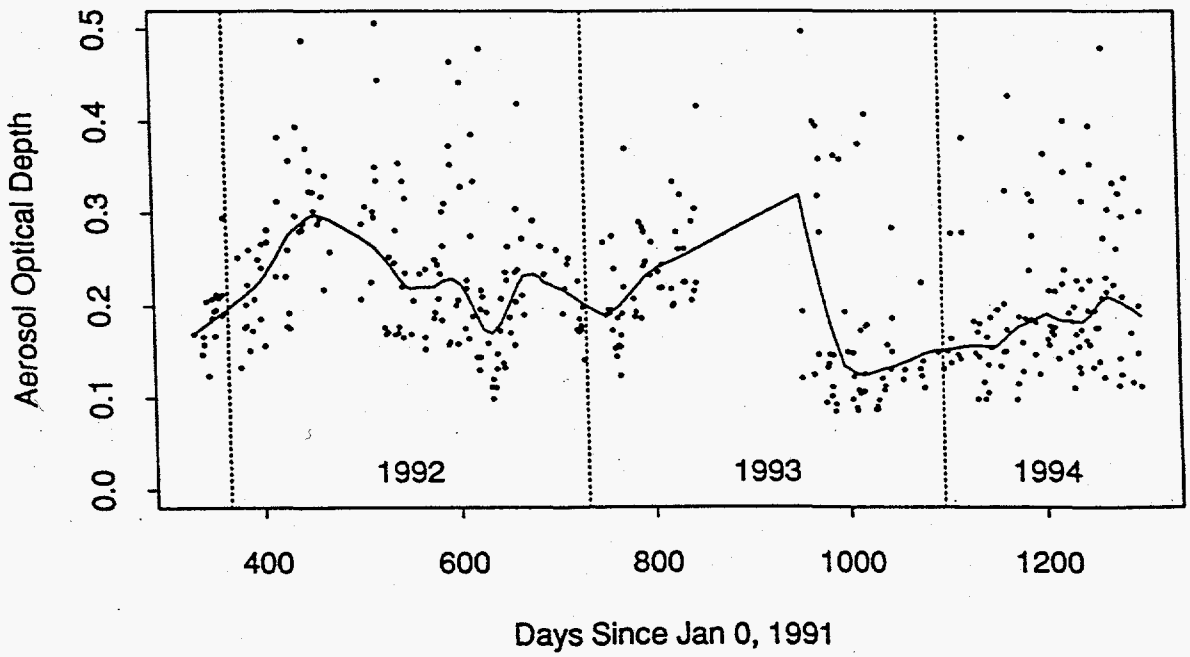


Figure 7 (top). Aerosol optical depth time series for Bluefield State College at 500 nm.
Figure 8 (bottom). Aerosol optical depth time series for Ill. State Water Survey at 500 nm.

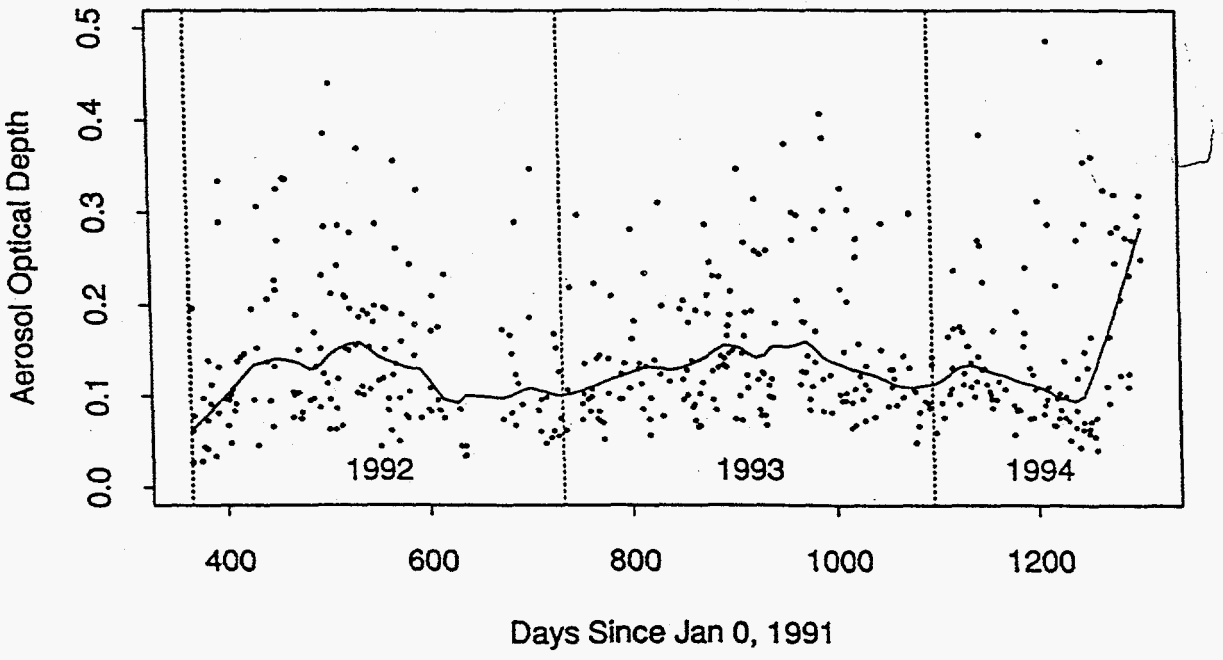


Figure 9. Aerosol optical depth time series for ASRC at 500 nm after removal of the Mount Pinatubo aerosol.